

Estimation and Management of Performance Limiting Factors in the Development of 1 kW Peak Power Pulsed Fiber MOPA at 1550 nm

Lalita Agrawal^{#,*}, Atul Bhardwaj[#], Dinesh Ganotra[@], and Hari Babu Srivastava[#]

[#]DRDO-Laser Science and Technology Centre, Delhi - 110 054, India

[@]Indira Gandhi Delhi Technical University for Women, Delhi - 110 006, India

*E-mail: lalitaagrawal@lastec.drdo.in

ABSTRACT

An all-fiber three-stage master oscillator power amplifier (MOPA), based on Erbium and Erbium-Ytterbium co-doped fibers, has been designed and developed. The performance of such a laser is primarily limited by amplified spontaneous emission (ASE), Yb bottlenecking, and non-linear effects. Other important factors, that need to be considered towards performance improvement, are fiber bend diameter and heat generated in the fiber. This paper describes the methodology for the estimation and management of these limiting factors for each amplifier stage. The work presented here is limited to the fibers which are commercially easily available, unlike customised Yb-free large mode area (LMA) Erbium-doped fibers, where very high peak and average powers are being reported due to the absence of Yb ASE. Presented experimental results and discussion shall be beneficial for the fiber laser amplifier designers. With suitable management, 1 kW peak power pulses of 30 ns duration at 200 kHz repetition rate have been achieved with 30 % optical efficiency. The collimated output of 6 W average power (limited by Yb ASE) with high beam quality ($M^2 \approx 1.6$) at 1550 nm can be employed for a variety of applications. By adding additional amplifier stages, power can be scaled further.

Keywords: Pulsed fiber MOPA; EYDF amplifier; ASE; Non-linear effects

1. INTRODUCTION

Pulsed Erbium and Erbium-Ytterbium co-Doped Fiber (EYDF) lasers /amplifiers are very attractive candidates for many long-range applications¹⁻³ like ranging, remote sensing, 3D imaging, and LIDAR, etc. They are not only eye-safe but have high atmospheric transparency also. In all-fiber architecture, they provide alignment-free, compact, and high beam quality laser. The performance of such a laser is limited by several factors like amplified spontaneous emission (ASE), non-linear effects, and Yb bottlenecking. Fiber bending and heat generation in the fiber are also required to be managed for performance improvement.

This paper describes the methodology for the estimation and management of these limiting factors for each amplifier stage. The work presented here is limited to the fibers which are commercially easily available, unlike customised Yb-free LMA erbium-doped fibers as mentioned in⁴⁻⁷ or multi-filament core fibers⁷. Inclusion of bulk optics such as gratings⁸ shall be also avoided to have a robust all-fiber configuration.

A brief description of various factors limiting the performance of an Er / Er-Yb pulsed fiber MOPA is given in the following section. Their estimation and management for the present configuration have been discussed stage-wise in subsequent sections.

1.1 Major performance limiting factors

Various factors that limit the performance of Er / Er-Yb pulsed fiber MOPA are described below.

1.1.1 Amplified Spontaneous Emission

In a fiber amplifier, noise due to spontaneous emission also gets amplified along with the signal. At high pump powers, this ASE becomes a major limiting factor, particularly in pulsed amplifiers⁹. Under CW pumping the inter-pulse ASE may lead to unwanted depletion of inversion before the arrival of signal pulse and may also cause inter-pulse self-pulsing and parasitic lasing. Such effects can be reduced¹⁰ in a multistage amplifier configuration with inter-stage ASE filters. A multistage amplifier configuration is also preferred to keep the amplifier gain ≈ 20 dB or less thus reducing ASE noise.

For many applications such as LIDAR and target illumination etc., operation at lower repetition rates (1-10 kHz) may be desired. At these rates, higher inversion can be created in the gain medium, enabling higher energy extraction. In actual conditions, at lower repetition rates, ASE affects the energy storage, and special techniques e.g. gating and pulsed pumping¹¹ are employed to mitigate inter-pulse ASE effects. At high rep rates, the time between the pulses thus ASE accumulation is automatically reduced.

The difference between measured power and calculated average power (through measurement of energy) gives a reasonable quantitative estimate of ASE power. One can also analyse the spectral and temporal profiles to estimate the ASE power. Measurement of Signal to Noise Ratio (SNR) provides a good estimate of ASE noise.

1.1.2 Yb- bottlenecking in Er-Yb co-Doped Fiber (EYDF)

Addition of Yb ion, in Erbium-doped fibers, improves the pump absorption, thus increases the efficiency of EYDF amplifiers¹². But under very strong pumping, excited Yb ions may not transfer energy quickly to the Er ions leading to Yb bottlenecking effect¹³ which causes emission from Yb energy levels. This parasitic lasing hampers the signal growth and may induce irreversible damage to various components. It was first proposed¹⁴ to have a controlled simultaneous laser oscillation near 1 μm for increasing the power level at 1.5 μm . After that, several other methods are being employed to suppress Yb parasitic lasing e.g. adding an auxiliary signal from the Yb band, which was experimentally¹⁵⁻¹⁶ and theoretically investigated¹⁷⁻¹⁸. A positive feedback loop for the Yb signal was also employed¹⁹⁻²¹ to overcome this problem.

In the present case, we have monitored the onset of Yb-ASE / parasitic lasing employing a dichroic mirror at the output to separate it from signal wavelength, and pump power is not increased further to work below the Yb ASE threshold.

1.1.3 Non-linear Effects

The small core size of fibers, to maintain a near single-mode transmission, leads to intense power density, which brings strong nonlinear effects such as stimulated Raman scattering (SRS) and stimulated Brillouin scattering (SBS) which can limit the maximum output power of fiber lasers²². Large-core or large mode area (LMA) fibers help in reducing optical intensity thus prevent these parasitic effects. LMA, however, leads to multimode propagation thus degrades beam quality.

In pulsed amplifiers, these effects may become much prominent due to the high peak powers involved. The SBS gain coefficient is an intrinsic property of the guiding medium and in silica-based fibers, its value is approximately 5.10^{-11} m/W, thus rendering SBS the lowest threshold nonlinear process in single-frequency CW fiber amplifiers. In comparison, the next lowest threshold phase-matched process is stimulated Raman scattering (SRS) which has a peak gain coefficient in silica fibers of less than 10^{-13} m/W. However, SBS effects may be neglected for broader linewidths²² and the SRS threshold can be estimated as²³

$$P_{thid}^{SRS} = \frac{16 \cdot \pi \cdot a^2}{g_R \cdot L} \cdot \Gamma^2 \cdot \ln(G) \quad (1)$$

where a is the core radius, g_R is Raman gain ($\approx 10^{-13}$ m/W for silica), G is amplifier gain factor (ratio: output/input), Γ is overlap factor (typical 80 %) and L is actual fiber length. To avoid the deleterious effects of SRS, it is recommended to work well below the estimated thresholds.

1.1.4 Heat Generation in Active Fiber

Fiber geometry has the advantage of a much higher surface-to-volume ratio than conventional solid-state laser media like rods and disks. Still, heat is generated in the active medium because of quantum-defect between pump and laser photons. Thermal effects may become significant at high input pump powers. Quantum defect in Er/Yb lasers is much higher than in only Yb doped fibers thus a larger amount of power is converted into heat. At high pump powers, heat generation in the fiber core may result in damage or degradation in the performance. In practice, damage to the fiber's outer coating becomes the main limiting factor. The outer coating not only acts as a protective layer but as the low index pump guiding layer also. Usually, the outer coating is a low refractive index fluorinated polymer that can withstand temperatures up to 150 °C - 200 °C before the onset of damage, and 80 °C is considered as the limit for long term reliability.

Heat generated inside the core is dependent on the quantum defect i.e. difference between pump and signal wavelengths and is given by the fraction $(1 - \lambda_p / \lambda_s)$ of pump input energy. It was proposed by Li²⁴, *et al.* that pump power, $P(z)$, decays exponentially along the length of fiber for cladding-pumped, Er-Yb-co-doped fiber laser, assuming flat hat pump profile in the core. The same expression was later employed by Ashoori²⁵, *et al.*, where the rate of heat generation per unit volume $q(Z)$ (in W/m³), inside the fiber, is given as

$$q(Z) = \frac{1}{L_{eff} \pi a^2} P_{in} \left(1 - \frac{\lambda_p}{\lambda_s} \right) e^{-\alpha z} \quad \text{for } r \leq a \quad (2)$$

$$\text{and } q(Z) = 0 \quad \text{for } a < r \leq c \quad (3)$$

Above expression is applicable for double-clad (cladding-pumped) fibers, so may not be used for preamplifier stages that are core-pumped. However, pump power in the initial stages is typically less than 1 W and can be managed without active cooling. Effective absorption (α) depends on the area ratio of core (πa^2) and cladding (πb^2), it is much less than the material absorption coefficient (α_m) at the pump wavelength, and is given by²⁵

$$\alpha = \alpha_m \frac{\pi a^2}{\pi b^2} NA_c \quad (4)$$

where NA_c is the numerical aperture of the core.

L_{eff} is the effective length which is smaller than the actual fiber length ' L ' because of fiber losses α and is given by²²

$$L_{eff} = \frac{(1 - e^{-\alpha L})}{\alpha} \quad (5)$$

Temperatures within different regions of fiber can be estimated using expressions given in²⁶. Temperature rise is maximum at fiber input end i.e. at $z = 0$ where the heat generation is maximum.

1.1.5 Fiber Bend Diameter

Fiber is usually designed to have a low loss for the propagating modes when it is straight but may exhibit significantly higher losses when bent. Fiber bending breaks the translational invariance of the refractive index in the

direction of propagation, thus power is lost from the modes near the bend²⁷. In the case of single-mode fibers, this applies to the fundamental mode and in multimode fibers applies to all bound modes. Bend loss can be significant for higher-order modes whilst being low for the fundamental mode as LP_{01} is the least sensitive to bend loss and for all higher modes, the bend-loss attenuation coefficient (in decibels per meter) depends exponentially on the radius of curvature^{27,28}. This feature can be utilised for discriminating higher-order modes in LMA fibers.

Bend loss estimation is rather involved and shall be reported in a separate publication. The estimation is based on numerical computation employing a full-vectorial Finite element method (FEM) mode-solver in the COMSOL Multiphysics software. Fiber geometry is created, and mode-solver is used to solve Maxwell's equations for relevant boundary conditions. The geometry is separated into core and cladding which are characterised by corresponding diameter and refractive index. For implementing losses into the simulation, a Perfectly Matched Layer, with a refractive index matched to the cladding region is used to realise the outer boundary region. Imaginary parts of the effective mode indices provide the modal power losses. One can estimate the suitable coiling diameter of the fiber that would result in >10 dB/m loss for LP_{11} and <0.1 dB/m loss for LP_{01} mode.

2. EXPERIMENTAL DETAILS

2.1 Seed Laser

To avoid SBS effects a directly modulated, broadband, high peak power Fabry-Perot, 14 - pin butterfly packaged, seed laser diode (OSI Inc., USA), emitting around 1550 nm, has been used as the master oscillator. Broader linewidth (≈ 8 nm) of the seed-laser was restricted to ≈ 2 nm (Fig. 1), employing two Band Pass Filters (BPF) in tandem, from Ascentta, USA, having a central wavelength of 1550 nm with ≈ 2 nm bandwidth at 0.5 dB and ≈ 6 nm bandwidth at 25 dB points. It has been found to result in a better overall performance with low spectral noise reducing the risk of parasitic lasing and inter-pulse self-pulsing¹⁰ in the power amplifier stage. The seed laser diode was operated in pulsed mode using a compact and versatile pulsed laser diode driver (Alphanov, France) that can generate peak currents up to 3 A with a wide range of pulse widths and pulse repetition rates. Operating pulse width and peak current of seed laser was fixed to 30 ns and 3 A respectively resulting in ≈ 25 mW peak power after two BPFs. Ideally energy per pulse thus peak power should remain almost the same over the whole range of repetition rates.

2.2 Fiber Amplifier Stages

To amplify ≈ 25 mW peak power pulses to kW level a total gain of ≈ 46 dB would be required. Considering the power amplifier stage to provide a typical gain of 15 dB, the rest 31 dB gain can be achieved by employing two preamplifier stages. Thus, a three-stage MOPA configuration (Fig. 2) was designed and implemented.

The first preamplifier stage consists of 2.3 m long single-mode Erbium-doped fiber (Nufern PM ESF 7/125), forward

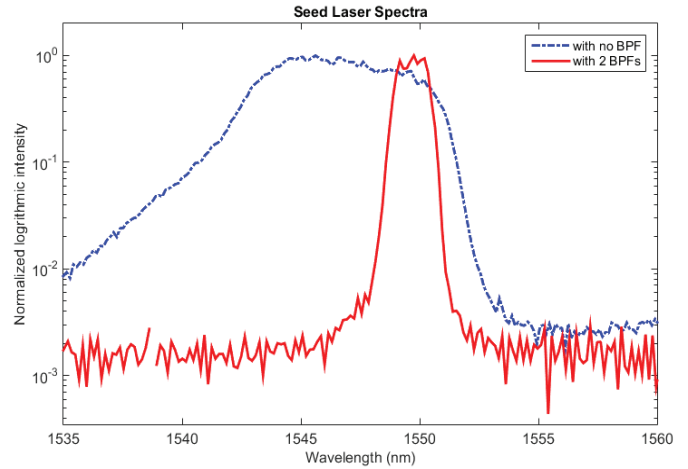


Figure 1. Seed laser spectra.

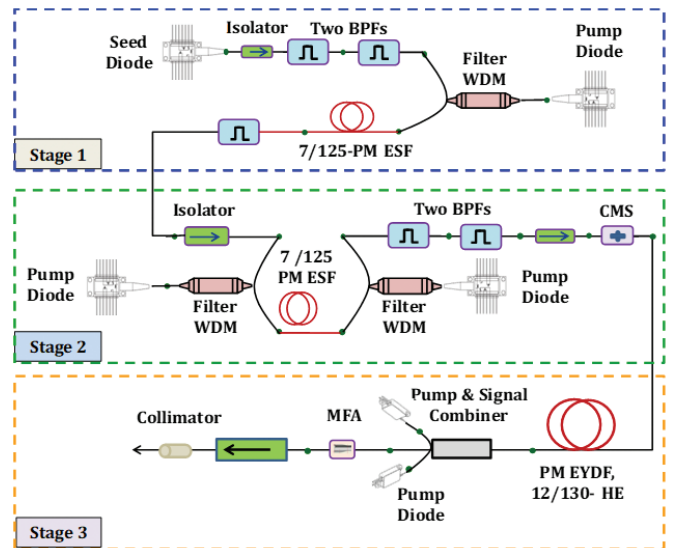


Figure 2. Schematic of three-stage MOPA configuration.

pumped by a CW pump diode emitting at 976 nm with ≈ 400 mW maximum power. For coupling the pump and signal powers into the fiber, a filter type Wavelength Division Multiplexer (WDM) has been used. The second amplifier stage is again of a similar fiber of ≈ 2 m length and is bi-directionally pumped with a total power of ≈ 740 mW. The second stage output is also filtered by two BPFs. The third amplifier stage is an EYDF LMA fiber (Nufern PM-EYDF-12/130-HE), which is backward pumped by two conduction-cooled 976 nm laser diodes of maximum 20 W power each (DILAS, Germany) employing a (2x1)+1 pump combiner (ITF technologies, Canada). Suitable isolators have been used between various stages to give protection against any back reflections. A Cladding Mode Stripper (CMS) has also been spliced after the second stage isolator for dumping the unused pump power from the third amplifier stage. A Mode Field Adapter (MFA) was employed to couple the output into an LMA fiber (25/300 μ m) of high-power handling (12 W) isolator with an integrated collimator (Agiltron, USA). Our application requires polarised output, however, due to the non-availability of a high extinction ratio polariser, Polarisation Extinction Ratio could not be measured presently.

Fiber lengths in preamplifier stages were optimised by the cut-back technique. Initially ≈ 4 m long fibers were taken and the length was cut-back in several small steps to maximise the output energy at 10 kHz repetition rate¹⁰. The fiber length for the EYDF amplifier stage was chosen for ≈ 10 dB pump power absorption. The cutback technique was not used to avoid wastage of fiber. For the 976 nm pump (absorption 8.1 dB/m), the active fiber length of 1.2 m was used.

3. RESULTS AND DISCUSSION

Experiments were carried out to evaluate the performance of each amplifier stage. The output from each amplifier stage was characterised before coupling to the next stage. Depending on the expected power levels, different variants of power meters (Ophir, Israel) were used. Laser pulses were monitored employing InGaAs based photodetector (Model No.1623, Newfocus, USA). For spectral analysis, an optical spectrum analyser (SHR-IR model, Solar, Belarus) was used.

3.1 Stage-1 Performance

Stage-1 was operated at a maximum pump power of 350 mW and the output power was measured at different repetition rates from 10 to 500 kHz. Peak powers were calculated by dividing average power with corresponding duty factors (product of pulse width and repetition rate). Calculating Peak powers in this way may not give exact values of peak powers particularly at low repetition rates. Thus, for estimation of inter-pulse energy one can employ the method suggested by Hernandez²⁹, *et al.* By the end of this work, we were able to have a high repetition rate energy meter by Gentec, Canada, thus final stage peak power was calculated by the measured pulse energy and pulse width. Stage gain was calculated for input peak power of 27 mW. Figure 3 depicts these performance parameters. It can be observed that output average power increases linearly from ≈ 10 mW to ≈ 25 mW up to 50 kHz repetition rate and after that power growth becomes very slow and it gets almost saturated beyond 150 kHz. Peak power and gain show the reverse trend. At low repetition rates, the gain is very high exceeding 30 dB which may result in high ASE content. At 500 kHz the gain ≈ 20 dB but keeping in view the power handling capability of second stage BPF and isolator (≈ 350 mW), the operation was limited to 200 kHz only (assuming ≈ 10 dB gain from the second stage). Calculated SRS threshold at 23.3 dB gain ($G \approx 216$) is ≈ 9.2 kW and at 30 dB ($G \approx 1000$) is ≈ 11.9 kW which are much above the corresponding peak powers (5.7 W and 36 W respectively).

Figure 4 shows the output average powers w.r.t input pump powers at different rep rates. At 200 kHz, ~ 35 mW power was achieved as compared to ≈ 10 mW at 10 kHz. Ideally, the measurement of energy could have given a better estimate of useful power without ASE. However, for stage-1 the pump power is not that high thus we expect useful power values may get only slightly modified at low repetition rates. For ASE noise estimation, spectral profiles were analysed at various repetition rates. Results indicate (Fig. 5) that signal to noise ratio (SNR) increases from 12 dB to 17 dB by increasing the repetition rate from 10 kHz to 200 kHz. Output pulses are shown in Fig. 6, at different repetition rates.

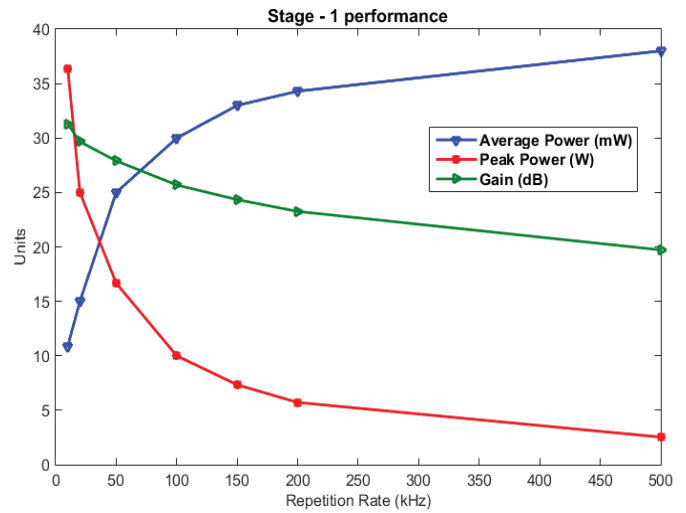


Figure 3. Stage-1 powers and gain at different repetition rates (for Y-axis units are shown in legend).

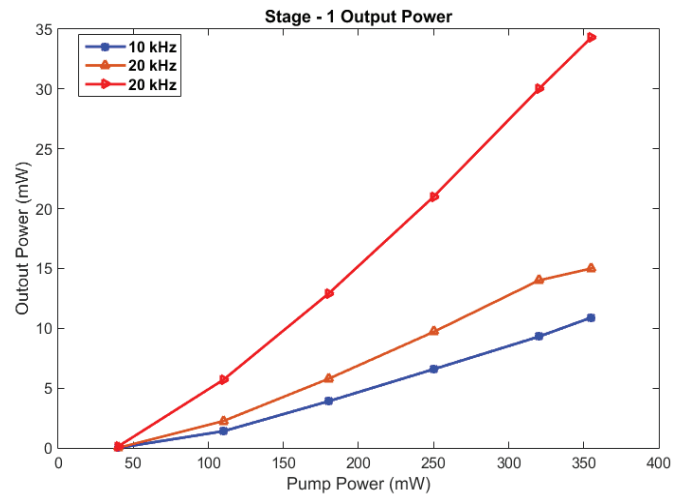


Figure 4. Stage-1 input-output powers at different repetition rates.

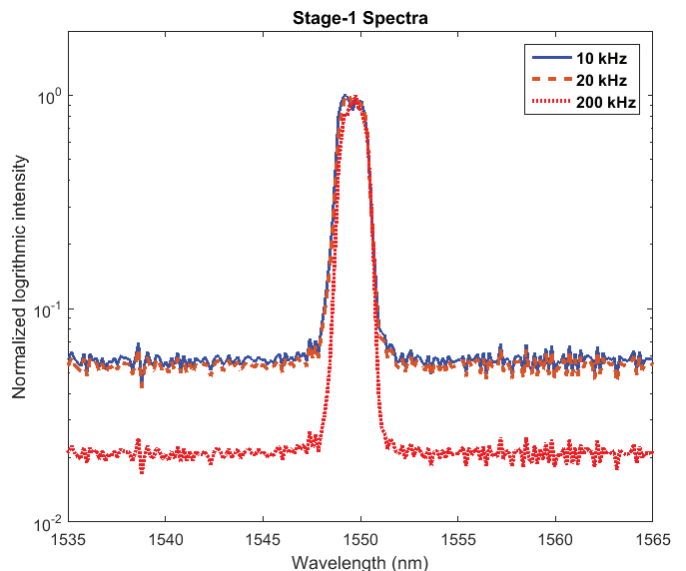


Figure 5. Stage-1 output spectra at different repetition rates.

3.2 Stage-2 Performance

The temporal performance of the second stage at different repetition rates was first analysed from angle cleaved doped fiber to avoid damage to BPFs with lower out-of-band power handling (≈ 300 mW) capability. The pulse profiles (Fig. 7) were taken with a photodetector placed very near to the output end (with safety precautions) for observing inter-pulse ASE near the bottom of laser pulses. Pulses were observed at a maximum total input power of ≈ 735 mW from two diodes. As can be seen, under CW pumping, significant inter-pulse ASE can build up at lower repetition rates. The operation was then carried out at 200 kHz only. Figure 8 depicts the spectra at two different pump powers showing a much better SNR value of ≈ 25 dB providing good signal input for the power amplifier stage. The average output power of 170 mW was achieved after the two BPFs and isolator (inset in Fig. 8).

3.3 Stage-3 Performance

For better performance of the power amplifier stage consisting of LMA EYDF fiber, several other factors besides intra band ASE are also required to be considered e.g. fiber bend radius, fiber cooling, and Yb ASE.

3.3.1 Fiber Bending and Cooling

Through fiber bend optimisation, we estimated the suitable coiling diameter of the EYDF (12/130) fiber to be ≈ 50 mm that would result in >10 dB/m loss for LP_{11} and <0.1 dB/m loss for LP_{01} mode. Thus, active fiber was coiled within specially designed spiral grooves on a water-cooled plate. Due to practical limitations, the fiber bend radius was kept constant in the present work, otherwise, one can observe the effect of fiber bending on the output beam quality.

Estimated heat load at the output end of the fiber (backward pumping, for $\alpha_m \approx 0.13$ m⁻¹ and $\alpha_m \approx 2.19 \cdot 10^{-4}$) was ≈ 6.2 W/m at 20 W input power for which active cooling was provided. During our experiments, we observed discoloration of the fiber (Fig. 9) after a repeated operation at high pump powers, we had to replace the fiber. For efficient heat removal, good thermal contact with the cold plate was provided using suitable interface material (Fig. 10). With efficient cooling, no discoloration or degradation was observed. To monitor the external temperature of active fiber, images were taken using a thermal camera (Model E-60, FLIR, USA).

3.3.2 Output Parameters of the Third Stage

Measurement of Yb ASE power was done from the angle cleaved MFA employing a dichroic mirror @45° angle to separate 1550 nm signal from ≈ 1000 nm Yb ASE band. Fig. 11 depicts the measured powers in two bands. As can be seen, initially the signal increases linearly with pump power but a deviation from the linear increase is observed after ≈ 25 W pump input. Correspondingly onset of Yb ASE is observed at ≈ 20 W pump power. Total pump power from the two diodes was limited to 35 W to avoid irreversible damage

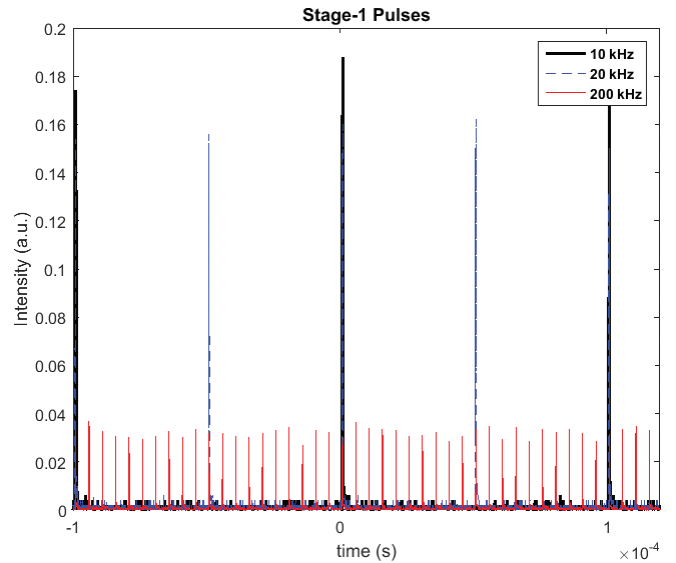


Figure 6. Stage-1 output pulses at different repetition rates.

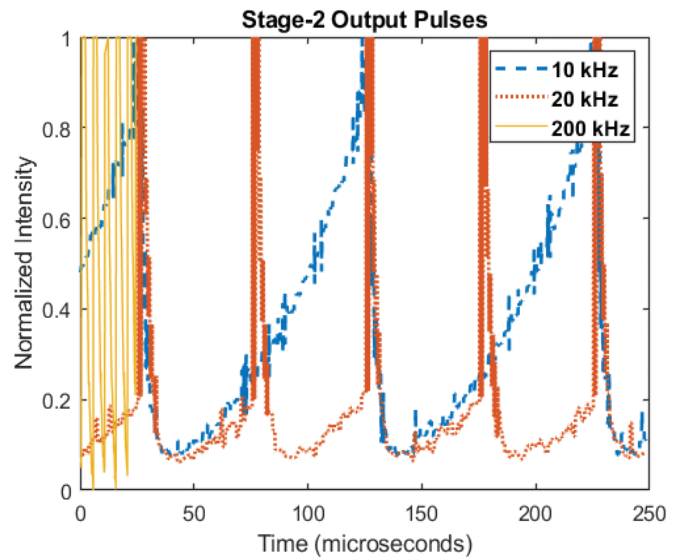


Figure 7. Stage-2 output pulses at different repetition rates.

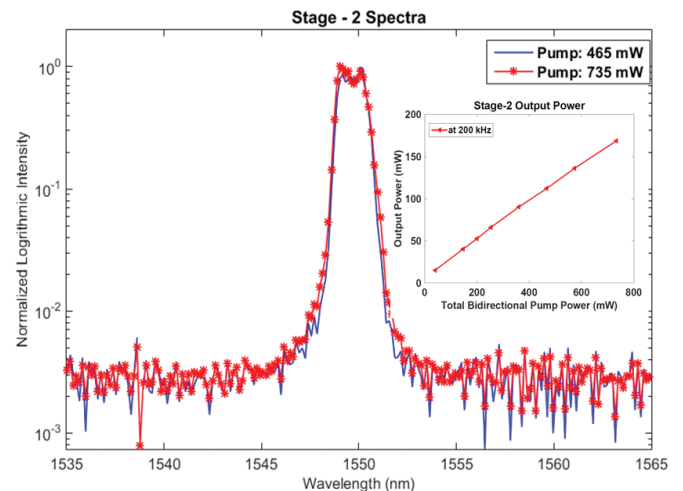


Figure 8. Stage-2 output spectra (power as inset) at 200 kHz repetition rate.

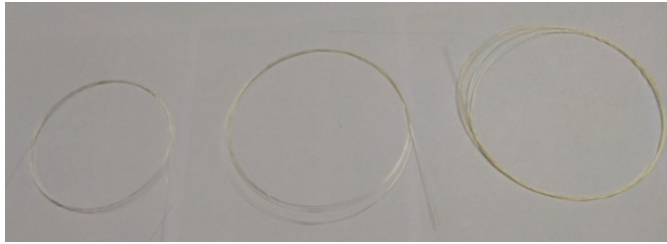


Figure 9. Picture showing a discoloration of EYDF fiber after a repeated operation at high pump powers.

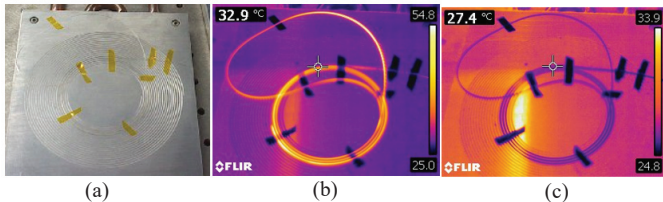


Figure 10. (a) Fiber mounted on a water-cooled plate in grooves, thermal image, (b) in absence of interface, and (c) in presence of interface material.

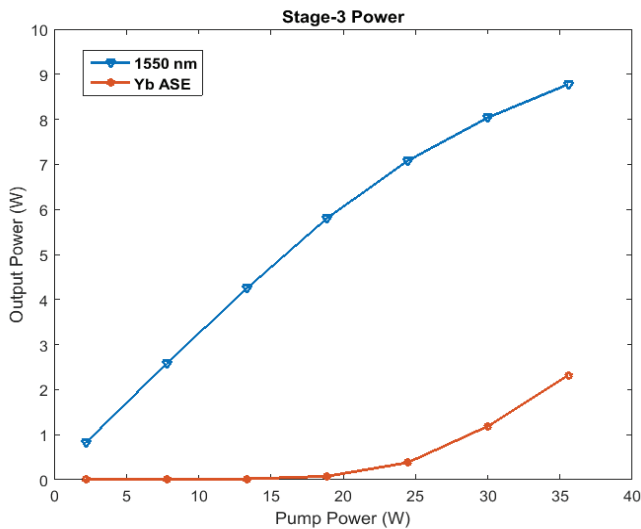


Figure 11. Stage-3 output power at 200 kHz.

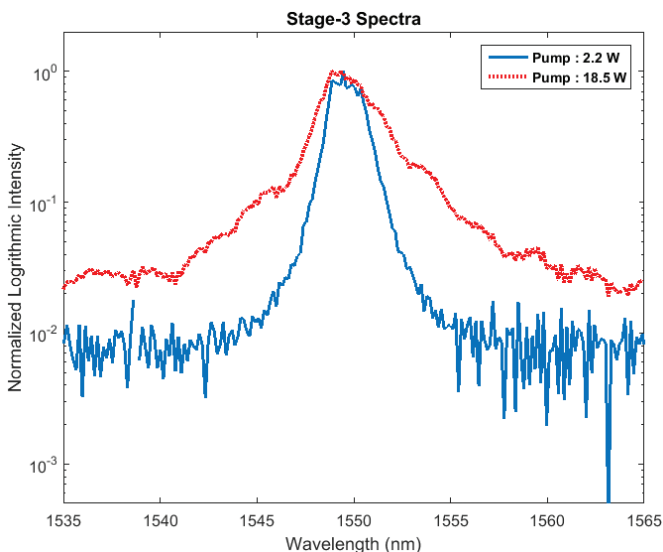


Figure 12. Stage-3 spectra at 200 kHz.

to the components. After splicing the isolator and collimator, pump power was further reduced to 20 W for protecting the isolator from high Yb ASE power. Figure 12 shows the final spectra with approximately 5 nm spectral width (3 dB). Employing suitable high-power handling BPF, in the future, this can be improved further.

Single laser pulse of 30ns duration and multiple pulses at 200 kHz repetition rate are shown in Fig. 13. Output pulse energy as measured by Mach-6, 200 kHz laser energy meter (Gentec, Canada) is depicted in Fig. 14. Average energy remains $\approx 30 \mu\text{J}$ with a standard deviation of $\approx 1.5 \mu\text{J}$, when the threshold of measurement was set to $4 \mu\text{J}$ so that only actual pulse energy is recorded, thus $\approx 1 \text{ kW}$ output peak power was achieved after the collimator.

Beam quality (Fig. 15) was measured by the beam squared system (Ophir (Spiricon), Israel) as $M^2_x:1.57$ and $M^2_y:1.56$.

Summary of final Er/ Er-Yb pulsed fiber MOPA parameters at $\sim 1550 \text{ nm}$ is given in Table 1

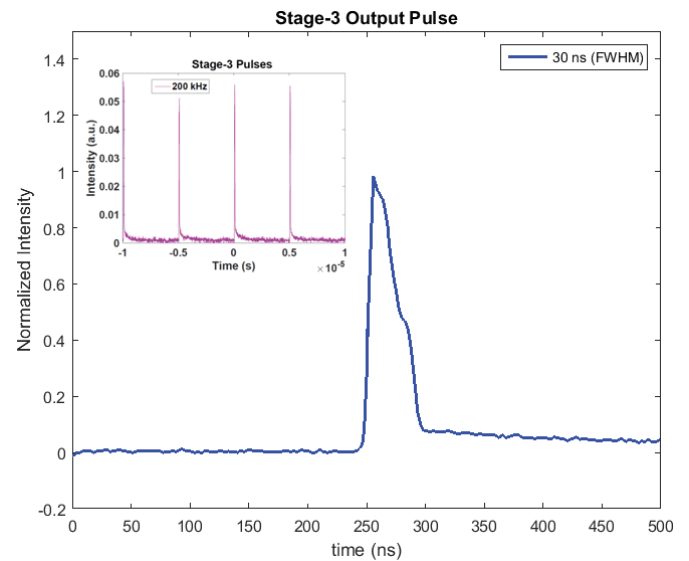


Figure 13. Stage-3 pulses at 200 kHz.

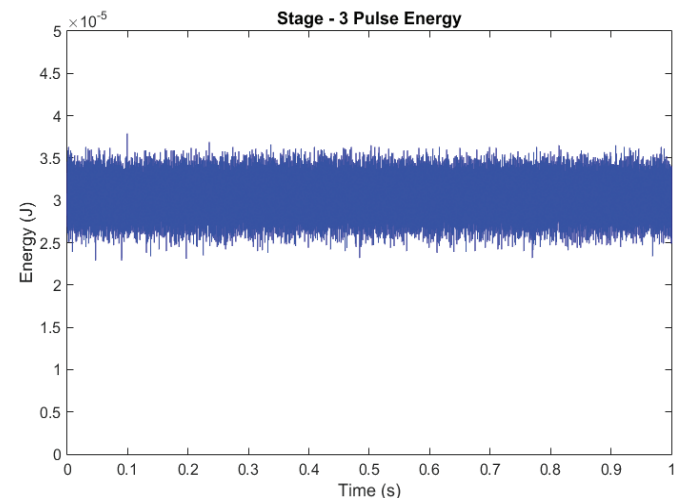


Figure 14. Stage-3 pulse energy at 200 kHz.

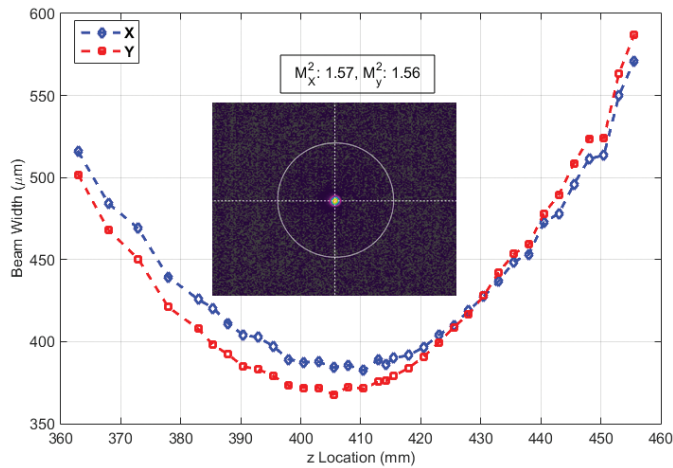


Figure 15. Beam quality and beam profile (inset) after stage-3.

Table 1. MOPA Performance parameters

Parameter	Value		
	Stage-1	Stage-2	Stage-3
Fiber core diameter	7 μm	7 μm	12 μm
Fiber length	2.3 m	2 m	1.2 m
Signal pulse width	30 ns	30 ns	30 ns
Signal repetition rate	200 kHz	200 kHz	200 kHz
Input signal average power	162 μW	35 mW	170 mW
Input signal peak power	27 mW	5.7 W	28.3 W
Input pump power (CW)	350 mW	735 mW	20 W
Output average power	35 mW	170 mW	6 W
Optical efficiency	10 %	23 %	30 %
Output peak power	5.7 W	28.3 W	1 kW
Amplification factor (G)	216	4.85	35.3
Gain	23.3 dB	6.8 dB	15.5 dB
SRS threshold	9.2 kW	3.1 kW	34.4 kW
SNR	17 dB	25 dB	17 dB
3 dB linewidth	$\sim 3\text{nm}$	$\sim 3\text{nm}$	$\sim 5\text{nm}$

4. CONCLUSIONS

Design details and experimental observations have been presented for an all-fiber three-stage master oscillator power amplifier (MOPA), based on Erbium and Erbium-Ytterbium co-doped fibers. 1 kW peak power pulses of 30 ns duration at 200 kHz repetition rate with 30 % optical efficiency have been achieved. The collimated output from this laser with 6 W average power (limited by Yb ASE) and high beam quality ($M^2 \approx 1.6$) at 1550 nm can be employed for a variety of applications. Special emphasis has been given to the estimation and management of performance limiting factors like ASE, non-linear effects, Yb bottlenecking, fiber coiling and cooling, etc. The simplest mitigation method is to either avoid or work below the onset of such deleterious effects. It is important to characterise each amplifier stage before coupling to the next stage, considering the power handling capabilities of various components. Damage may not be always visible immediately but may degrade the performance slowly and affect the reliability of the laser. Presented experimental results and discussion shall be beneficial for the laser designers working in this area.

REFERENCES

- Canat, G.; Lombard, L.; Dolfi, A.; Valla, M.; Planchat, C.; Augère, B.; Bourdon, P.; Jolivet, V.; Besson, C.; Jaouën, Y.; Jetschke, S.; Unger, S.; Kirchhof, J.; Gueorguiev, E. & Vitre, C., High brightness 1.5 μm pulsed fiber laser for lidar: From fibers to systems. *Fiber Integr. Opt.*, 2008, **27**, 422–439. doi: 10.1080/01468030802269431
- Holmen, L.G.; Rustad, G. & Haakestad, M.W., Eye-safe fiber laser for long-range 3D imaging applications. *Appl. Opt.*, 2018, **57**, 6760. doi: 10.1364/AO.57.006760
- Cariou, J.P.; Augere, B. & Valla, M., Laser source requirements for coherent lidars based on fiber technology. *C. R. Phys.*, 2006, **7**, 213–223. doi: 10.1016/j.crhy.2006.03.012
- Kotov, L.; Likhachev, M.; Bubnov, M.; Medvedkov, O.; Lipatov, D.; Guryanov, A.; Zaytsev, K.; Jossent, M. & Février, S. Millijoule pulse energy 100-nanosecond Er-doped fiber laser. *Opt. Lett.*, 2015, **40**, 1189. doi: 10.1364/OL.40.001189
- Kotov, L. V.; Likhachev, M.E.; Bubnov, M.M.; Medvedkov, O.I.; Yashkov, M. V.; Guryanov, A.N.; Lhermite, J.; Février, S. & Cormier, E. 75 W, 40% efficiency single-mode all-fiber erbium-doped laser cladding-pumped at 976 nm. *Opt. Lett.*, 2013, **38**, 2230. doi: 10.1364/OL.38.002230
- Khudyakov, M. M.; Bubnov, M. M.; Senatorov, A.K.; Lipatov, D.S.; Likhachev, M.E.; Rybaltovsky, A.A.; Butov, O. V.; Gur'yanov, A.N. & Kotov, L. V. Cladding-pumped 70-kW-peak-power 2-ns-pulse Er-doped fiber amplifier, in A.L. Carter, I. Hartl (Eds.), *Fiber Lasers XV: Technol. Syst.*, SPIE, 2018, **10512**, 1051216. doi: 10.1117/12.2290837
- Canat, G.; Jetschke, S.; Unger, S.; Lombard, L.; Bourdon, P.; Kirchhof, J.; Jolivet, V.; Dolfi, A. & Vasseur, O. Multifilament-core fibers for high energy pulse amplification at 1.5 μm with excellent beam quality. *Opt. Lett.*, 2008, **33**, 2701. doi: 10.1364/OL.33.002701
- Zhao, Z.; Xuan, H.; Igarashi, H.; Ito, S.; Kakizaki, K. & Kobayashi, Y. Single frequency, 5 ns, 200 μJ , 1553 nm fiber laser using silica-based Er-doped fiber. *Opt. Express*, 2015, **23**, 29764–29771. doi: 10.1364/OE.23.029764
- Sintov, Y.; Glick, Y.; Kopolowitch, T. & Nafcha, Y. Extractable energy from erbium-ytterbium co-doped pulsed fiber amplifiers and lasers. *Opt. Commun.*, 2008, **281**, 1162–1178. doi: 10.1016/j.optcom.2007.10.043
- Agrawal, L. & Ganotra, D. Suppression of parasitic lasing and inter-pulse self-pulsing in a pulsed Erbium-Ytterbium co-doped fiber amplifier. *Appl. Phys. B*, 2020, **126**, 14. doi: 10.1007/s00340-019-7368-8
- Klopfer, M.; Block, M.K.; Deffenbaugh, J.; Fitzpatrick, Z.G.; Urioste, M.T.; Henry, L.J. & Jain, R. Control of pulse format in high energy per pulse all-fiber erbium /ytterbium laser systems, in: Kudryashov, A. V.; Paxton, A.H. & V.S.

- Iichenko (Eds.). *Laser Resonators, Microresonators, and Beam Control XIX*, 2017, p. 100901N.
doi: 10.1117/12.2248910
12. Townsend, J.E.; Barnes, W.L. & Crubb, S.G. Yb³⁺ sensitised Er³⁺ doped silica optical fibre with ultra high transfer efficiency and gain. *In MRS Proceedings*, 1991, **244**, 143.
doi: 10.1557/PROC-244-143
 13. Loh, W.H.; Samson, B.N.; Dong, L.; Cowle, G.J. & Hsu, K. High-performance single-frequency fiber grating-based erbium/ytterbium-codoped fiber lasers. *J. Lightwave Technol.*, 1998, **16**, 114–118.
doi: 10.1109/50.654992
 14. Jeong, Y.; Yoo, S.; Codemard, C.A.; Nilsson, J.; Sahu, J.K.; Payne, D.N.; Horley, R.; Turner, P.W.; Hickey, L.; Harker, A.; Lovelady, M. & Piper, A. Erbium:Ytterbium codoped large-core fiber laser with 297 W continuous-wave output power. *IEEE J. Sel. Top. Quantum Electron.*, 2007, **13**, 573–579.
doi: 10.1109/JSTQE.2007.897178
 15. Kuhn, V.; Weßels, P.; Neumann, J. & Kracht, D. Stabilization and power scaling of cladding-pumped Er:Yb-codoped fiber amplifier via auxiliary signal at 1064 nm. *Opt. Express*, 2009, **17**, 18304.
doi: 10.1364/OE.17.018304
 16. Sobon, G.; Kaczmarek, P.; Antonczak, A.; Sotor, J. & Abramski, K.M. Controlling the 1 μm spontaneous emission in Er/Yb co-doped fiber amplifiers. *Opt. Express*, 2011, **19** 19104.
doi: 10.1364/OE.19.019104
 17. Han, Q.; Ning J. & Sheng, Z. Numerical investigation of the ASE and power scaling of cladding-pumped Er–Yb co-doped fiber amplifiers. *IEEE J. Quantum Electron.*, 2010, **46**, 1535–1541.
doi: 10.1109/JQE.2010.2052789
 18. Han, Q.; He, Y.; Sheng, Z.; Zhang, W.; Ning, J. & Xiao, H. Numerical characterization of Yb-signal-aided cladding-pumped Er:Yb-codoped fiber amplifiers. *Opt. Lett.*, 2011, **36**, 1599.
doi: 10.1364/OL.36.001599
 19. Sobon, G.; Kaczmarek, P.; Antonczak, A.; Sotor, J. & Abramski, K.M. Controlling the 1 μm spontaneous emission in Er /Yb co-doped fiber amplifiers. *Opt. Express*, 2011, **19**, 19104.
doi: 10.1364/OE.19.019104
 20. Sobon, G.; Sliwinska, D.; Kaczmarek, P. & Abramski, K.M. Er/Yb co-doped fiber amplifier with wavelength-tuned Yb-band ring resonator. *Opt. Commun.*, 2012, **285**, 3816–3819.
doi: 10.1016/j.optcom.2012.05.018
 21. Zhao, X.; Han, Q.; Wang, D.; Hu H.; Ren, K.; Jiang, J. & Liu, T. Optimal design of high-power cascade co-pumping Er/Yb-codoped fiber lasers. *Opt. Lett.*, 2019 **44**, 1100.
doi: 10.1364/OL.44.001100
 22. Agrawal, G.P. Chapter 1 - Introduction, in: *Nonlinear Fiber Optics (Fourth Edition)*, 2006.
doi: 10.1016/B978-012369516-1/50001-7
 23. Dawson, J.W.; Messerly, M.J.; Beach, R.J.; Shverdin, M.Y.; Stappaerts, E.A.; Sridharan, A.K.; Pax, P.H.; Heebner, J.E.; Siders, C.W. & Barty, C.P.J. Analysis of the scalability of diffraction-limited fiber lasers and amplifiers to high average power. *Opt. Express*, 2008, **16**, 13240.
doi: 10.1364/OE.16.013240
 24. Li, L.; Li, H.; Qiu, T.; Temyanko, V. L.; Morrell, M. M. & Schülzgen, A. 3-Dimensional thermal analysis and active cooling of short-length high-power fiber lasers. *Opt. Express*, 2005, **13**, 3420–3428.
doi: 10.1364/OPEX.13.003420
 25. Ashoori, V. & Malakzadeh, A. Explicit exact three-dimensional analytical temperature distribution in passively and actively cooled high-power fiber lasers. *J. Phys. D: Appl. Phys.*, 2011, **44**, 355103.
doi: 10.1088/0022-3727/44/35/355103
 26. Fan, Y.; He, B.; Zhou, J.; Zheng, J.; Liu, H.; Wei, Y.; Dong, J. & Lou, Q. Thermal effects in kilowatt all-fiber MOPA. *Opt. Express*, 2011, **19**, 15162.
doi: 10.1364/OE.19.015162
 27. Marcuse, D. Influence of curvature on the losses of doubly clad fibers. *Appl. Opt.*, 1982, **21**, 4208.
doi: 10.1364/AO.21.004208
 28. Koplów, J. P.; Kliner, D.A.V & Goldberg, L. Single-mode operation of a coiled multimode fiber amplifier. *Opt. Lett.*, 2000, **25**, 442 – 445.
doi: 10.1364/OL.25.000442
 29. Hernandez, P.G.R.; Belal, M.; Baker, C.; Pidishety, S.; Feng, Y.; Friebele, E.J.; Shaw, L.B.; Rhonehouse, D.; Sanghera, J. & Nilsson, J. Efficient extraction of high pulse energy from partly quenched highly Er³⁺ doped fiber amplifiers. *Opt. Express*, 2020, **28**, 17124–17142.
doi: 10.1364/OE.385426

ACKNOWLEDGMENT

The authors are thankful to all members of the Pulsed Laser Sources (PLS) group of LASTEC for their support during experiments.

CONTRIBUTORS

Ms Lalita Agrawal completed her BSc (H) Physics and M.Sc. (Physics) with electronics from the University of Delhi in 1985 and 1987, respectively. She is working as Scientist G and heading the Pulsed Laser Sources Group at Laser Science & Technology Centre (LASTEC), Delhi. She is a recipient of DRDO Laboratory Technology Group Awards in 2002 and 2007 for significant contributions towards various diode-pumped solid-state laser technologies and recently in 2018 for pulsed fiber laser technology. Currently, she is pursuing her Ph.D. (Physics) from Indira Gandhi Delhi Technical University for Women, Delhi.

In the present study, she has carried out the research work and written the full manuscript including all graphs and figures.

Mr Atul Bhardwaj completed his BSc (H) Physics in 1996 and MSc (Physics) in 1998 from the University of Delhi. He is working as Scientist F at Laser Science & Technology Centre (LASTEC), Delhi. He is a recipient of DRDO Laboratory Technology Group Awards in 2007 and 2018 and Laboratory Scientist of The Year Awards in 2009 and 2017 for significant

contributions towards various diode-pumped solid-state and pulsed fiber laser technologies. His current research interests include theoretical and experimental studies on high peak power pulsed fiber lasers.

In the present study, he provided support in the experimental and theoretical work. He has also contributed towards the revision of the manuscript as per reviewers' comments.

Dr Dinesh Ganotra has done his PhD from the Indian Institute of Technology, Delhi, and post-doc from the University of Arizona, USA. He is currently working as an Associate Professor at Indira Gandhi Delhi Technical University for Women, Delhi. His research interests include digital image processing, computer vision, neural networks, pattern recognition, and speech processing.

In the current research work, he supervised the work and provided valuable guidance and suggestions for improving the quality of the research paper.

Mr. Hari Babu Srivastava, Outstanding Scientist and Director of Laser Science and Technology Centre (LASTEC), Delhi, is an alumnus of IIT Roorkee and IIT Kanpur from where he obtained his B.E. and M.Tech. degrees in Electrical Engineering, respectively. Currently spearheading various technology and product development initiatives in the areas of high-power lasers, laser spectroscopy, and laser countermeasure applications. He is a recipient of the DRDO Technology Group Awards for his contribution towards various DRDO programs.

In the present study, he reviewed and approved the manuscript for publication.